TeleTA: Teleoperation System with Tactile Feedback aimed at Presentation of the Physical Contact on Entire Robot Arm Surface to the Human Operator

Dzmitry Tsetserukou
University of Tokyo
7-3-1 Hongo, Bunkyo-ku, Tokyo
dima_teterukov@ipc.i.u-tokyo.ac.jp

Susumu Tachi
University of Tokyo
7-3-1 Hongo, Bunkyo-ku, Tokyo
http://tachilab.org/

Abstract

The paper focuses on the teleoperation system designed to achieve high level of maneuverability of robot arm in unstructured and dynamic environment. The human operator directs the robot arm to the target position, while manipulator sensory system provides safe physical interaction with environment. In order to achieve awareness of collision and to support operator with valuable information, we elaborated approach to contacting force vector calculation and delivering this information to the operator's skin through tactile display. The analysis of different types of haptic display showed that increasing tactile information density does not obviously lead to the quality of information presentation. Thus, we concentrated on the development of a new type of apparatus that accounts for effectiveness of the information presentation, power consumption, ergonomics, and usability for particular teleoperation task. The application of proposed design can be extended for VR systems, wearable information systems, etc.

1. Introduction

Telerobotic systems allow a robot manipulator to be controlled from a physically separate location. Robot arm is commanded by human operator supervising the advance of operation. The operator has to execute skilful manoeuvres to avoid collisions and direct the robot to its goal position. In virtual environment, the simulated bodies have predefined coordinates, and many effective collision detection algorithms have been already elaborated. When we consider the real indoor environments, known obstacles (e.g. chairs, tables, etc.) and unknown obstacles (persons approaching the robot, unmapped environment, etc.) change their location dynamically. Moreover, the object shape, speed and position can also alter in unpredictable way. In order to provide the robot with detailed real-time environment view it is imperative to use sensor data.

In many remote-controlled systems visual, force, and audio channels deliver operator the information about scene. The main issues in using visual feedback are narrow visible area and occlusion of view by robot arm. Another challenge is significant time delay in such applications of telerobotics as controlling the robot in space station from the earth or in case when operator and robot are located at a distant places. Failing feedback cues user cannot avert unexpected collision. Even if the human operator has clear picture what is happening in remote side, he has inherent difficulty with planning collision-free motion of the entire manipulator body [1].

The only effective solution of such challenge is to endow robot arm with ability to safely contact with environment in an autonomous manner. Lumelsky *et al.* [2] proposed to cover manipulator with a sensitive skin capable of detecting nearby objects. An array of infrared proximity sensors delivers the information about obstacles obstructing arm motion to the control system. The algorithm of motion planner manoeuvres the robot arm avoiding impact.

Recently proposed sophisticated imaging systems, such as stereovision and laser scanning, presume usage of expensive detectors and complex signal processing techniques. They sense only narrow space around the robot body. The concept of sensor array composed of ultrasonic rangefinders and infrared detectors is described in [3]. Researchers are pursuing the goal of the development of a robust proximity sensor system with application in mobile robotics, taking advantage of high performance/cost ratio of the components and low computational demands of the detection method. Due to the specular nature of ultrasonic waves reflection, the only objects normally located to the sensor acoustic axis can be accurately detected. As it comes to infrared sensor, one of the most important problems is limited measuring performance. The amplitude from the infrared sensor largely depends on reflectivity of the object and changes with the target distance in non-liner manner. There is high possibility that proximity sensors fail to detect obstacle along the robot trajectory. In this case an immediate vicinity of the target can mislead robot control system invoking the abrupt change in the speed resulting in harm of the environment.

We argue that robot should be mainly controlled not to avoid the collision but rather to ensure safe contact

ICAT 2008
Dec. 1-3, Yokohama, Japan
ISSN: 1345-127

interaction with environment through gathering the comprehensive information about objects (shape, stiffness, texture, location, fixation, etc.). Conventional approaches to handle the interaction between a manipulator and environment are based on impedance control of a robot arm according to applied force vector measured at the manipulator wrist [4]. However, the rest parts of the robot body (forearm, elbow, upper arm, shoulder, and torso) are presenting significant danger not only to human being, but also to the robot structure itself. Safety can be improved by intentionally introducing compliance at the mechanical design level [5]. However, elements with high compliance negatively affect the performance of a robot.

The paper focuses on the teleoperation system **TeleTA** (**Tele**operetion system with wearable **T**actile display on the operator arm surface providing **A**wareness about slave robot collision) designed by us to achieve high level of maneuverability of robot arm in unstructured dynamic environment and to perform cooperative tasks with humans in a safe manner. We announce several distinctive contributions in this paper. New remote robot and sensory system for the operation in cluttered environment were developed. Distributed optical joint torque sensors and local admittance controllers endow our robot arm with the distinctive capability of safe interaction with surroundings along entire manipulator surface. The developed remote robot is equipped with the tactile sensor enabling to detect coordinates of the contact point. The force vector direction on the entire robot arm surface (including joints) can be calculated from the values of joint torques and contact point coordinates. The algorithm of the force vector calculation is given in the paper.

Although the teleoperated robot can contact with obstacle in a safe manner, unawareness of the user about contacting force and actual position still remains safety problems. It is because of limits on joint ranges and possible torque sensor overloading. Besides, in the case when operator fulfills violent maneuver the human cooperating with robot can be injured. These facts raise the second question: delivering the tactile cues to the operator.

The issues of optimal representation of contact information are discussed in the paper. The developed ergonomic bracelet-shaped tactile display BraTact intended for presenting the force vector information to the operator skin in intuitive way is described.

The remainder of paper is structured as follows. Section 2 presents the teleoperation system TeleTA. Section 3 describes the robot sensory system and data processing algorithms. The approach to calculation of contact force vector and experimental results are introduced in Section 4. In Section 5, we focus on the techniques of tactile information presentation and detail the development stages of haptic display BraTact. Section 6 concludes the paper and discusses the future work.

2. Teleoperation system TeleTA

The teleoperation system TeleTA aimed at performing the cooperative tasks with humans and operating in unstructured environment is shown in Fig. 1.

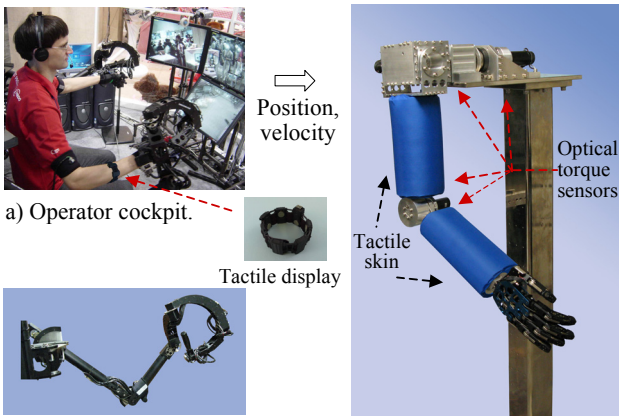

a) Operator cockpit. b) Master arm. c) Remote robot.

Figure 1: Robot teleoperation system TeleTA.

Master side (Fig. 1(a)) includes exoskeleton robot arm with 6 DOF (Fig. 1(b)) to direct the slave robot arm and tactile display BraTact to present cutaneous stimulation when collision or contact with object is detected. The orientation of the human elbow is controlled by the tilt sensor.

From the safety point of view, to minimize injures in case of collision, most of the parts of teleoperated robot arm (Fig. 1(c)) were manufactured from aluminium alloys to obtain as much lightweight structure as possible. The robot links were designed in round shape to reduce impact force. The distribution of robot arm joints replicates the human arm structure in order to make it easy to operate using kinesthetic sensation.

To remove mechanical subsystems without disassembling the main structure when the failures do occur, we have been using a modular approach while designing anthropomorphic robot arm. Therefore, we selected CSF-series gear head type of harmonic drive instead of compact and lightweight component one. The harmonic drive offers such advantages as accurate positioning, high torque capability, torsional stiffness, and high single stage ratios. Developed teleoperated robot arm has 4-DOF: Roll, Pitch, Yaw joints of a shoulder, and Pitch joint of an elbow. Such orthogonal disposition of the axes simplifies the installation of the torque sensors and motor drives into the joints, allowing thus avoidance of application of additional belt driven actuators. The 3D CAD model of the developed arm and coordinate systems based on Denavit-Hartenberg convention are represented in Fig. 2.

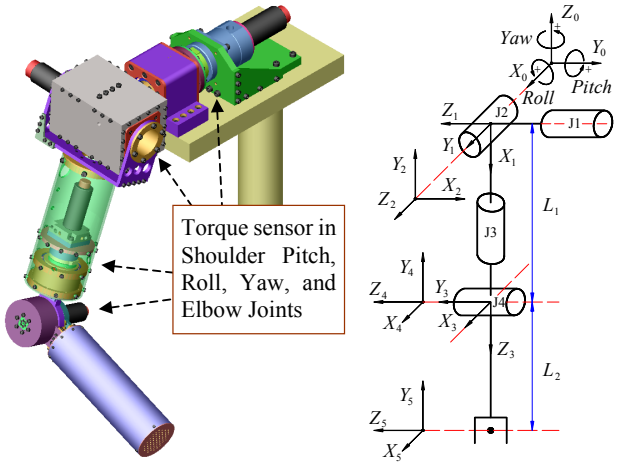

Figure 2: 3D CAD arm model and coordinate systems.

Each joint is equipped with optical torque sensor directly connected to the output shaft of harmonic drive. The sizes and appearance of the arm were chosen so that the sense of incongruity during interaction with human is avoided. We kept the arm proportions the same as in average height Japanese male, aged 25: upper arm length L_1 - 0.308 m; upper arm circumference - 0.251 m (diameter 0.080 m); forearm length L_2 - 0.241 m; forearm circumference - 0.189 m (diameter 0.06 m). The motors are equipped with magnetic encoders having 512 pulses per revolution.

3. Robot sensory system

Proposed sensory system patterns on the human tactile system. Our sense of touch can be separated into kinesthetic and coetaneous. Kinesthetic stimulations, produced by forces exerted on body, are sensed by mechanoreceptors in the joints, tendons, and muscles enabling us to estimate forces being applied to body. When we hold a heavy object in a palm, its weight produces torques in the wrist, elbow, and shoulder joint. Each muscle generates a torque at a joint that is the product of its contractile force and its moment arm at that joint to balance gravity force, as well as, mechanical constraints of joints, inertial forces, and contact forces [6]. Thus, we can manipulate the object and feel its weight. On the contrary, mechanoreceptors in the skin layers are responsible for cutaneous stimulation sensation. Different types of tactile corpuscles allow us sensing thermal properties of object, pressure, vibration frequency, pain, and stimuli localization. Merkel cells and Meissner's corpuscles provide the most precise localization of touch, as they have smallest receptive fields and are also more sensitive to pressure applied by a small probe. Very fine spatial resolution of the human skin allows performing tactile discrimination of surface texture and shape by fingertips. For practical implementation of the proposed approach we developed sensory system of the robot arm that includes optical torque sensors distributed into each joint (to measure applied force) and tactile skin (to detect contact point).

The robot arm is covered with Kinotex tactile sensor measuring the pressure intensity through amount of backscattered light falling on photodetector [7]. The sensitivity, resolution, and dynamic range of this artificial skin are comparable to those of a human. The taxels displaced with 21.5 mm in X and 22 mm in Y direction make up 6x10 array.

In technical specifications of the Kinotex sensor, the ability of force measurement is indicated. However, the following shortcomings complicate the accurate measurement of the applied force: temperature dependency of the transducer constant, fragility while mechanical overloading, large hysteresivity, high non-linearity of the output, limited sensing range, etc. Additionally, the tactile sensors detect and measure the spatial distribution of forces perpendicular to a predetermined sensory area and, hence, cannot evaluate the vector components of applied force. Thus, the most appropriate application of such tactile sensors is the contact area recognition and the measurement of relative pressure distribution in the contact region on the robot body surface. The task of load measurement is accomplished by the developed optical torque sensors enabling torque measurement with high accuracy.

In order to recognize the contact region, we employed the watershed algorithm, an image processing segmentation technique that splits an image into areas based on the topology of the image [8]. The adopted algorithm is processed as follows: departing from the local maximum, the new taxel is included into the contact area only if within the 3x3 array surrounding it there is an other taxel of greater or equal pressure intensity already included into the water stream.

The accurate estimation of the contact point can be obtained by computing the center of gravity of the contact pattern $c(x_c,y_c)$ of the neighborhood Ω by:

$$c(x_c,y_c)=\left(\frac{\sum_{x,y\in\Omega} x_i f_i(x_i,y_i)}{\sum_{x,y\in\Omega} f_i(x_i,y_i)},\frac{\sum_{x,y\in\Omega} y_i f_i(x_i,y_i)}{\sum_{x,y\in\Omega} f_i(x_i,y_i)}\right), \quad (1)$$

where $f_i(x_i,y_i)$ is the pressure intensity level of the taxel i with coordinates (x_i,y_i).

The artificial skin sensor generates the data stream processed by the developed Win32 C++ application. The program analyses the tactile pattern and calculates the number of contacts and the center of gravity of the contact pattern based on the pressure distribution information. The example of contact area image obtained by using Kinotex skin is presented in Fig. 3.

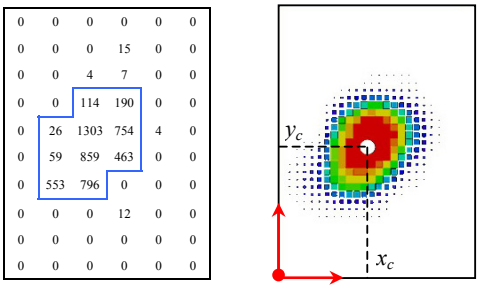

a) Digital image b) Visual image

Figure 3: Representations of the contact area.

In order to facilitate the realization of torque measurement in each arm joint, we developed optical torque sensors. The novelty of our method is application of the ultra-small size photointerrupter (PI) RPI-121 as sensitive element to measure relative motion of sensor components. The dimensions of the PI (3.6 mm × 2.6 mm × 3.3 mm) and its weight of 0.05 g allow realization of compact design. The optical torque sensor is set between the driving shaft of the harmonic transmission and driven shaft of the joint (Fig. 4). When the load is applied to the robot joint, the magnitude of the output signal from the PI corresponds to the exerted load.

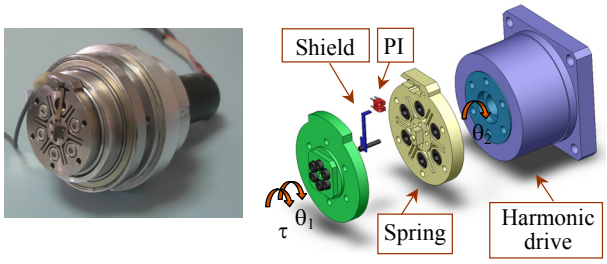

Figure 4: Torque sensor of the elbow joint.

The spring members attached to the first, second, and third/fourth joints were designed to measure torque of ± 12.5 Nm, ± 10.5 Nm, ± 4.5 Nm, and have resolution of 10.77 mNm, 9.02 mNm, and 4.31 mNm, respectively. Each sensor was calibrated by means of attachment of reference weights to the lever arm. Non-linearity of 2.5 % of Full Scale was calculated using maximum deviated value from the best-fit line.

The developed optical torque sensors have high dependability, good accuracy (even in electrically noisy environment), low price, compact sizes, light weight, and easy manufacturing procedure.

4. Calculation of contact force vector

The proposed algorithm of computing the force vector at any contact point on entire teleoperated robot arm employs information about the contact point coordinates and joint torque values. The forces ${}^{i}f_i$ acting in the coordinate system of each joint produce moments ${}^{i}n_i$ (Eq. (2)). The joint torques are derived by taking Z component of the moments applied to the link (Eq. (4)).

$$ {}^{i}n_i = {}_{i+1}^{i}R\,{}^{i+1}n_{i+1} + {}^{i}P_{C_i} \times {}^{i}F_i + {}^{i}P_{i+1} \times {}_{i+1}^{i}R\,{}^{i+1}f_{i+1} \quad (2) $$

$$ {}^{i}f_i = {}_{i+1}^{i}R\,{}^{i+1}f_{i+1} + {}^{i}F_i \quad (3) $$

$$ \tau_i = {}^{i}n_i^{T}\,{}^{i}\hat{Z}_i \ , \quad (4) $$

where ${}_{i+1}^{i}R$ is the matrix of rotation between links i+1 and i calculated using Denavit-Hartenberg notation; ${}^{i}P_{i+1}$, ${}^{i}P_{Ci}$ are the vectors locating the origin of the coordinate system i+1 in the system i, and contact point, respectively; ${}^{i}F_i$ is the contact force.

Let us consider the case when force is applied to the upper arm of the robot. Using the Eq. (2), (3) we have:

$$ {}^{2}n_2 = \begin{bmatrix} 0 \\ L_{F2} \\ 0 \end{bmatrix} \times \begin{bmatrix} F_{2x} \\ F_{2y} \\ F_{2z} \end{bmatrix} = \begin{bmatrix} L_{F2}F_{2z} \\ 0 \\ -L_{F2}F_{2x} \end{bmatrix}; $$

$$ {}^{1}n_1 = \begin{bmatrix} s_2 & c_2 & 0 \\ 0 & 0 & 1 \\ c_2 & -s_2 & 0 \end{bmatrix} \begin{bmatrix} L_{F2}F_{2z} \\ 0 \\ -L_{F2}F_{2x} \end{bmatrix} = \begin{bmatrix} L_{F2}F_{2z}s_2 \\ -L_{F2}F_{2x} \\ L_{F2}F_{2z}c_2 \end{bmatrix}. \quad (5) $$

The components of the applied force vector and force magnitude are derived from:

$$ F_{2x} = \tau_2 / (-L_{F2}) \ ; \ F_{2z} = \tau_1 / (L_{F2}c_2) \ ; $$

$$ F_2 = \sqrt{(F_{2x})^2 + (F_{2z})^2} \ . \quad (6) $$

The value of the applied force projection on the axis Y is not required because the upper arm cannot move in this direction. For the case when the force acts on the forearm we have the following algorithm to obtain the contact force vector:

$$ F_{4y} = \frac{(\tau_2 + F_{4z}(L_{F4}c_3c_4 + L_2c_3) + F_{4x}(L_{F4}s_3 + L_2s_3c_4))}{(L_2s_3s_4)} $$

$$ F_{4x} = \tau_4 / L_{F4} \ ; \ F_{4z} = \tau_3 / (L_{F4}s_4), \quad (7) $$

where c_2, c_3, c_4, s_3, and s_4 are abbreviations for $\cos(\theta_2)$, $\cos(\theta_3)$, $\cos(\theta_4)$, $\sin(\theta_3)$, and $\sin(\theta_4)$, respectively; L_2, L_{F2}, and L_{F4} are the lengths of the moment arms.

To evaluate the feasibility of the proposed approach, the experiments were conducted. During the experiment, the object was moved along the upper arm surface according to the curve shown in Fig. 5(c). While contacting, the torque values measured at the first and second joint (τ_1, τ_2) vary in

accordance with Fig. 5(a). The contact force vector projections (F_{2x}, F_{2z}) and force vector length F_2 obtained from Eq. (6) are represented in Fig. 5(b). The trajectory of the end point of the contact force vector is shown in Fig. 5(d).

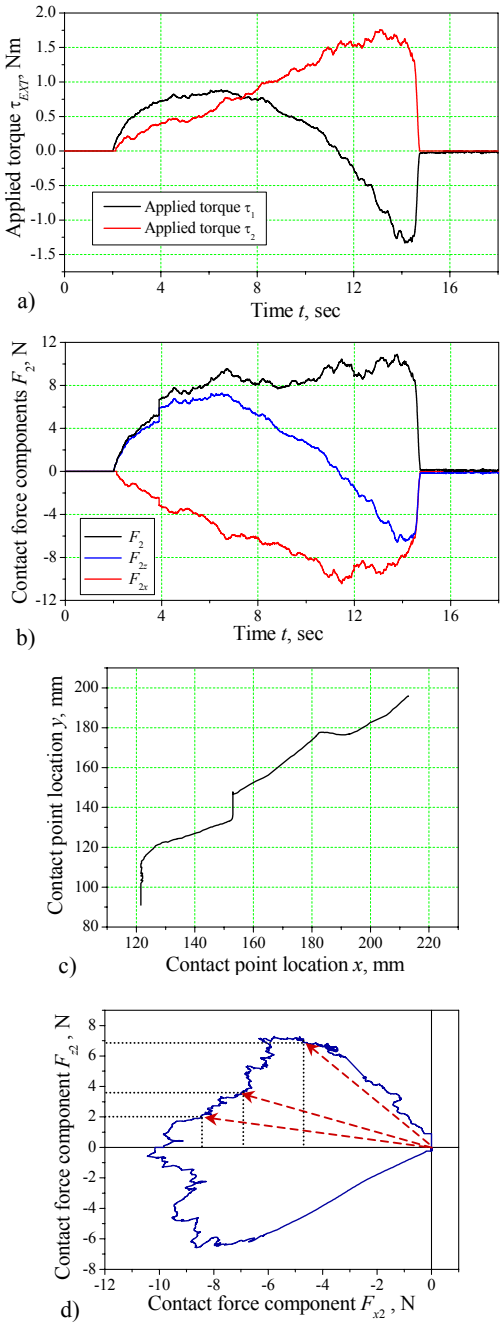

Figure 5: Experimental results.

Robot sensory system and proposed algorithm have demonstrated the ability of contact force vector calculation.

5. Development of the ergonomic tactile display BraTact

While interacting with objects in VR or manipulating the robot, human sensory system has to process a plenty of information cues. Generally, users of VR or teleoperation systems extensively utilize vision and hearing channels. In some cases haptic displays can present the information in more intuitive way.

In order to deliver the sense of object touch to the operator, the force-feedback devices [9, 10] (generating kinesthetic stimuli) and tactile-feedback system [11] (evoking cutaneous stimuli on local area of the skin) are widely applied. The devices of former type are able to exert strong forces on human body and limit user motion in a natural manner. However, they are cumbersome, have narrow workspace, and enable to generate force only at the human hand. When it comes to the contact presentation on the human arm, tactile displays are preferable ones. They can convey contact cues [12], direction [13] and distance [14] information. Recently, haptic gadgets displaying information on a large area of the human body are gaining increased attention by researchers.

In [15], the authors pursue the goal of ensuring the safety during low visibility helicopter landing. This paper introduces the study on alternative approach of flight information presentation through tactile display instead of visual display. The tactile suit comprises belts with 31 tactors around the waist and a column of 21 tactors on the back. This tactile display supplies the pilot with information on groundspeed and altitude. Experimental results showed that landing manoeuver performance in degraded visual environment was significantly improved when groundspeed and altitude were presented on tactile display. Yang *et al.* [16] presented vibro-tactile wear endowing human with tactile perception of interaction object in VR and allowing to direct the motion of the limbs. Tactile display has cylindrical fashion to be worn on the torso of a user with array of 60 vibration motors. From experimental results researchers concluded that design of tactile feedback system should account for what factor is more critical: information accuracy or object presence. In [17], reconfigurable, wearable system TactaVest for delivering vibro-tactile stimuli aimed at enhanced human-computer interaction is presented. The tactors were mounted on the body at the locations having a high probability of contacting virtual object (namely, shoulder, elbow, belt placement area and breast). The authors made valuable proposal for improvement of garments design, tactor placement, and wiring.

It can be seen from the papers presented above that, typically, the huge amount of sensors are arranged in regular grid pattern and attached to the human body. The researchers faced the question: is it really necessary to

employ many tactors making device heavy, with complicated wiring system and uncomfortable design? Is increasing number of tactors the effective way to convey tactile information?

It should be mentioned here, that heavy tactile display placed on the arm surface degrades the mobility and increases joint muscle loading. Moreover, the higher density of conveyed tactile information the less attention user pays to target task (move in VR, observe situation, manipulate the object, direct the robot arm, etc.), thus leading to important information loss. Therefore, we have to find out the approach to effective presentation of tactile information.

For the time present, insignificant attempts were made to optimize the design of tactile display in such a way that it can be informative, ergonomic, lightweight, wearable, intuitively understandable in use, comfortable in wearing, with small power consumption and friendly design. In this paper, we propose the tactile display design that satisfies mentioned demands for delivering the contact force vector information to the operator.

During teleoperation user has to move arm in extensive way. Additional weight on the arms will cause the overloading of the operator muscles. On the other hand, display should not restrict the motion range of the human arm. Therefore, the main issue we have to face in designing the tactile display is to make it compact and lightweight. In contrast to the method of covering the whole arm surface with tactile garment, we are proposing to use two tactile bracelets worn on the middle parts of the forearm and upper arm. The force vector is coded as follows: (1) the tactor operating on the arm surface represents the force direction, and (2) the magnitude of the contact force is conveyed by vibration intensity.

The developed tactile bracelet BraTact incorporates six vibration motors with holders linked by elastic band. Proposed shape takes advantage of the facts that we already used to wear bracelet-shaped watches and accessories, and that such shape of the tactile display can fit to the humans of different sizes. It should be noted that in traditional design all tactors are attached to one piece of stretchy substrate [16] and wrapped by tight fitting wristband or T-shirt that allows vibrations to propagate along the structure deteriorating the tactor localization by user. In our design each tactor is separated from neighboring units that enhances the discrimination of the tactile pattern.

Several attempts were made to explore the human tactile patterns for effective communication with mobile devices. It was found that identification accuracy at the nine tactor locations on the dorsal side of the wrist ranges from 22% to 76% [18]. The participants of the study were generally better at identifying the tactor location across the back of the arm than along the arm. Chen *et al.* [19] examined the human ability to localize a single vibration source on dorsal and volar sides of the forearm near wrist. For the experiments a 3-by-3 tactor array was placed on the dorsal and volar parts of the wrist, respectively. An important finding was that on average only 4 tactor locations could be correctly identified on both sides of the wrist.

Despite the conclusion mentioned above, we use number of tactors exceeding the recommended in [19]. Based on our assumption that the tactile sensitivity in the middle parts of the human forearm or upper arm is higher than that of a wrist due to the size of circumference, we decided to design BraTact for these parts. Moreover, to enhance the localization ability, we arrange the tactors in a zigzag pattern. To ensure the close contact of the tactor with the skin and the adaptation to different sizes of the potential users, the holders are connected by elastic band. The layout of tactile system BraTact is shown in Fig. 6.

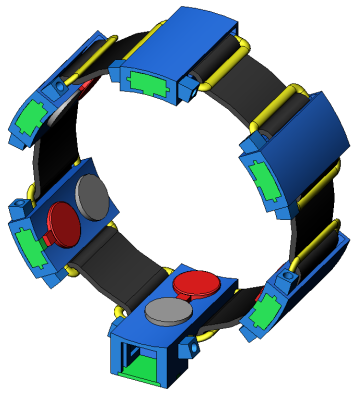

Figure 6: Tactile display BraTact.

It was reported that maintaining permanent contact of the tactor with the skin is crucial issue [20]. The holder was designed in such a way that flat vibration motors protrude and contact arm directly. The 3D prototype of the tactor unit is presented in Fig. 7.

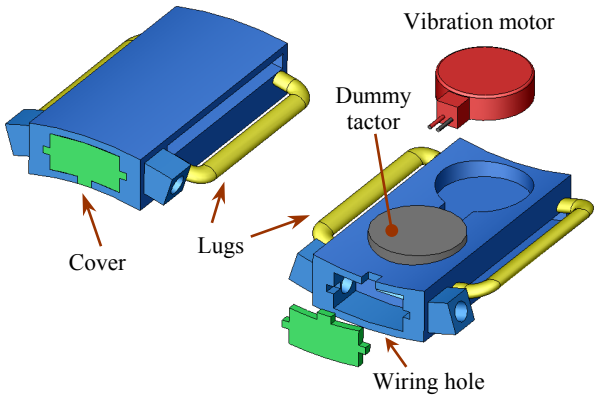

Figure 7: The link of the tactile bracelet.

The inner surface of the holder has concave profile to

match the curvature of human arm surface. The curvature of the holder surface of 39 mm was calculated on the basis of the forearm circumference value of average Japanese male (it equals to 246 mm). To balance the position of the link on the skin, the additional dummy tactor is provided.

The most fragile parts of the holder are lugs intended for tactor link fixation on flexible band. To find out the optimal sizes of the lug cross-section, we performed FEM analysis. The initial data are material of the holder (ABS plastic) and maximum force applied to the lug by stretched band (4 N). The results of analysis of plastic holder using FEM demonstrate FEM model (Fig. 8(a)), displacement in m (Fig. 8(b)), strain (Fig. 8(c)), and von Mises stress $\sigma_{VonMises}$ in N/m^2 (Fig. 8(d)).

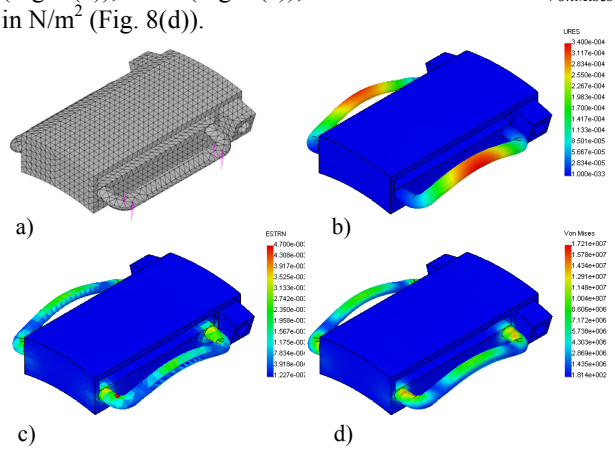

Figure 8: FEM analysis results.

Factor of safety of 2.5 was derived based on the maximum von Mises stress criterion. Thus, designed structure can guarantee overloading protection. The holders were produces by using 3D printer. The disassembled link and tactile bracelet are shown in Fig. 9.

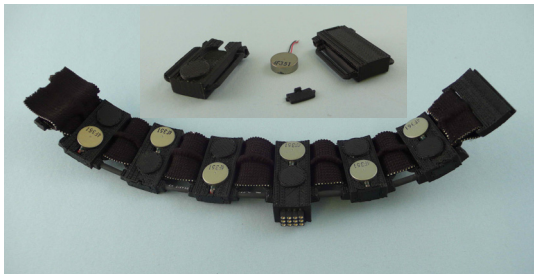

Figure 9: Prototype of the tactile bracelet.

To supply the power to the tactors, thin wires with overall diameter of 0.5 mm were used. The flexible tubes wrap wires protecting them from breaking. Compact connector socket was designed to unite vibration motor wiring with control board.

It can be seen form Fig. 10 that the developed BraTact display is compact and fits the arm very well.

Figure 10: BraTact attached to the human arm.

The small flat coreless vibration motors FM34F with diameter of 12 mm and thickness of 3.4 mm produce tactile stimulation on human skin [21]. They have operating voltage range of 2.5-3.5 V, corresponding frequency range of 181-236 Hz, and vibration quality of 1.8 G. The control signal is generated by PC, based on information about calculated force vector. A/D board feeds cue to the motor driver hardware that supplies corresponding voltage to the vibration motor (Fig. 11).

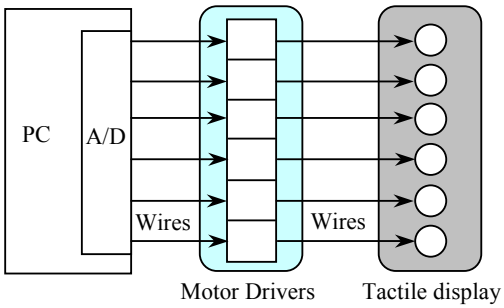

Figure 11: Control system of BraTact.

We use non-inverting amplifier to control the current of the vibration motor. The results of calibration of one tactor are presented in Fig. 12. During experiment we increased the input voltage of operational amplifier and recorded the current value in vibration motor circuit.

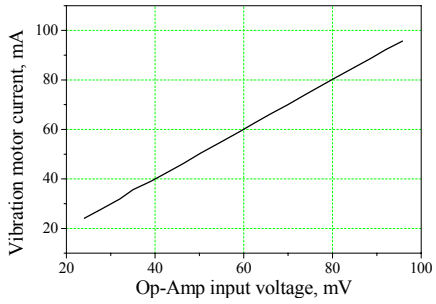

Figure 12: Control system of BraTact.

The control box with vibration motor drivers is shown in Fig. 13. To connect the driver box with tactile display the

lightweight shielded wire cable was deployed.

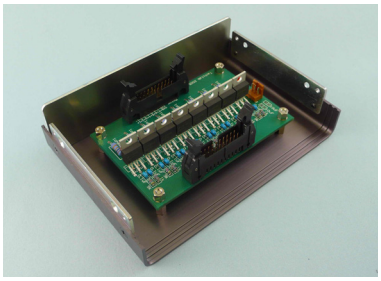

Figure 13: Control box.

The initial intensities of the tactors were adjusted to be equal. Through controlling the vibration motor current we change vibration motor rotational speed and, hence, vibration intensity.

6. Conclusions and future research

The increasing complexity of tasks performed by teleoperation systems requires to deliver and display tactile information to the human operator effectively in order to ensure safe interaction with environment. The sensory system of the developed slave robot supports the local admittance controllers with information on exerted force to accomplish compliant interaction. We argue that to present the interaction information effectively the usage of only two bracelets on upper and lower arms is better solution than employment of large grid of tactors on the human arm. According to our approach, the contact state can be presented by force vector. The direction of the force perpendicular to the arm surface is represented by location of the tactor; and force magnitude is represented by this tactor vibration intensity.

Our future study will be directed to the detailed investigation of the force vector perception. First, the discrimination of the tactors will be examined through user study. Then, we will conduct study on contacting force magnitude presentation through assignment of different vibration intensities. We are also considering designing the compact tactile displays for delivering the tactile information to the user's fingers.

Acknowledgments. The research is supported in part by a Japan Society for the Promotion of Science (JSPS) Postdoctoral Fellowship for Foreign Scholars.

References

[1] V. Lumelsky. On human performance in Telerobotics. IEEE Transaction on Systems, Man, and Cybernetics, 21(5): 971–982, 1991.

[2] V. J. Lumelsky, M. S. Shur, and S. Wagner. Sensitive skin. IEEE Sensors Journal, 1(1): 41–51, 2001.

[3] A. M. Sabatini, V. Genovese, E. Guglielmelli, A. Mantuano, G. Ratti, and P. Dario. A low-cost, composite sensor array combining ultrasonic and infrared proximity sensors. In Proc. IEEE/RSJ Int. Conf. on Intelligent Robots and Systems, Pittsburgh, 2003, pp. 120–126.

[4] F. Caccavael, C. Natale, B. Siciliano, and L. Villani. Six-DOF impedance control based on angle/axis representation. IEEE Transaction on Robotics and Automation, 15(2):289–300, 1999.

[5] A. Bicchi, and G. Tonietti, Fast and soft arm tactics: dealing with the safety-performance trade-off in robot arms design and control. IEEE Robotics and Automation Magazine, 11(2):22–33, 2004.

[6] E. R. Kandel, J. H. Schwartz, and T. M. Jessell. Principles of Neural Science. McGraw-Hill, New York, 2000.

[7] Optic fiber tactile sensor kinotex. Nitta Corporation. On-line available: http://www.nitta.co.jp/

[8] J. Serra. Image Analysis and Mathematical Morphology. Academic Press, London, 1982.

[9] PHANTOM line of haptic devices. On-line available: http://www.sensable.com

[10] CyberGrasp system. On-line available: http://www.immersion.com

[11] J.B.F. van Erp, and H.A.H.C. van Veen. A multi-purpose tactile vest for astronauts in the international space station. In Proc. Int. Conf. EuroHaptics, Dublin, 2003, pp. 405–408.

[12] R. D. Howe, D.A. Kontarinis, and W. J. Peine. Shape memory alloy actuator controller design for tactile displays. In Proc. 34th IEEE Conf. on Decision and Control, Vol. 4, 1995, pp. 3540–3544.

[13] H.A.H.C. van Veen, and J.B.F. van Erp. Providing directional information with tactile torso displays. In Proc. Int. Conf. EuroHaptics, Dublin, 2003, pp. 471–474.

[14] R.W. Cholewiak. The perception of tactile distance: Influences of body site, space, and time. Perception, 28(7):851–875, 1999.

[15] C. Jansen, A. Wennemers, W. Vos, and E. Groen. FlyTact: A tactile display improves a helicopter pilot landing performance in degraded visual environment. In Proc. Int. Conf. EuroHaptics, Madrid, 2008, pp. 867–875.

[16] U. Yang, Y. Jang, and G. J. Kim. Designing a vibro-tactile wear for "close range" interaction for VR-based motion training. In Proc. Int. Conf. on Artificial Reality and Telexistence, Tokyo, 2002, pp. 4–9.

[17] R. W. Lindeman, Y. Yanagida, H. Noma, and K. Hosaka. Wearable vibrotactile system for virtual contact and information display. Virtual Reality, 9:203–213, 2006.

[18] I. Oakley, Y. Kim, J. Lee, and J. Ryu. Determining the feasibility of forearm mounted vibrotactile displays. In Proc. Int. Symp. on Haptics Interfaces for Virtual Environment and Teleoperator Systems, Arlington, 2006, pp. 27–34.

[19] H-Y. Chen, J. Santos, M. Graves, K. Kim, and H. Z. Tan. Tactor localization at the wrist. In Proc. Int. Conf. EuroHaptics, Madrid, 2008, pp. 209–218.

[20] A. Rupert. An instrumentation solution for reducing spatial disorientation mishaps. IEEE Engineering in medicine and Biology Magazine, 19(2):71–80, 2000.

[21] T. Yamaguchi. Flat coreless vibrator motor using magnetic latching power. U. S. Patent No. 6 246143, 2001.